

Use of ESPI to evaluate the effect of orthodontic mini-implant thread design on bone strain

Bryan J. Houlberg, DDS

A thesis submitted in partial fulfillment
of the requirements for the degree of
Master of Science in Orthodontics

Oregon Health & Science University
Portland, Oregon

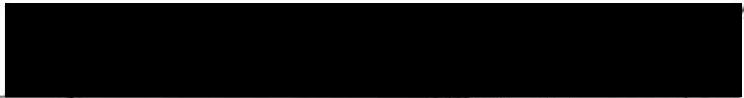
November, 2010

Use of ESPI to evaluate the effect of orthodontic mini-implant thread design on bone strain

Bryan J. Houlberg

Master of Science in Orthodontics Research Advisory Committee:

Signature: _____

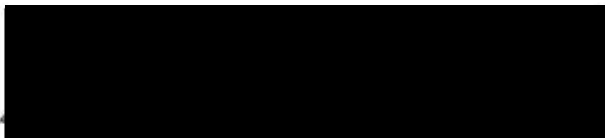


Date: 14-Dec-10

John C. Mitchell, PhD
Professor

Department of Biomaterials, School of Dentistry
Oregon Health and Science University

Signature: _____

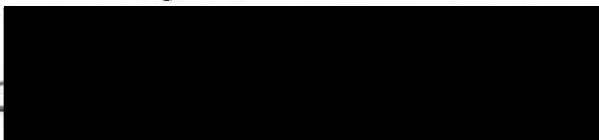


Date: 14-Dec-10

David A. Covell, Jr., PhD, DDS
Department Chair

Department of Orthodontics
Oregon Health and Science University

Signature: _____

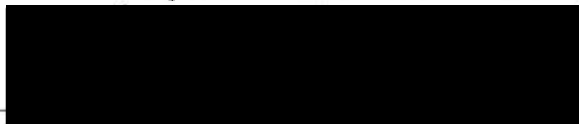


Date: 15-Dec-2010

Larry Doyle, DDS
Program Director

Department of Orthodontics
Oregon Health and Science University

Signature: _____



Date: 28-DEC-2010

Donald D. Duncan, PhD
Professor

Department of Electrical and Computer Engineering
Portland State University

Acknowledgements

Thank you to my project mentor, Dr. John Mitchell, for helping me organize the project, complete it in a timely manner, hash through my manuscript and thesis presentation, and helping me figure things out for myself, instead of just telling me the answer.

Thank you to the members of my committee from the Orthodontics Department, Dr. Dave Covell and Dr. Larry Doyle, for early guidance in selecting an avenue for research, and for their constructive advice for my manuscript and thesis presentation.

Thank you to Dr. Donald Duncan who knows and understands ESPI better than I ever will. Without your troubleshooting, problem solving, and advice during the testing procedure, we never could have fine-tuned the setup enough to get results.

Thank you to Todd Groesbeck, a now 3rd year dental student, for being my research partner, and for working hand in hand with me on the study design, test procedure, and analysis of what we found.

Thank you to Dr. Holly Grimslid, my big sib in the residency program, and Steve George, another now 3rd year dental student, for laying the groundwork for this study with your own study using ESPI and evaluating OMIs with and without collars.

Thank you to Dr. Jack Fisher for supplying the mini-implants for this study and being willing to help with anything we needed materials-wise.

Thank you to Dr. Mansen Wang for your help with the statistical analysis.

Thank you to Dr. Sean Kirkpatrick for trusting us enough with your very expensive, highly technical ESPI equipment so we could use it for our study.

Thank you to my family for dealing with me through the hours and hours I've spent on this project.

TABLE OF CONTENTS

	<u>Page</u>
List of Figures	6
List of Tables	7
Manuscript:	
Title Page	8
Abstract	9
Introduction	10
Materials and Methods	12
Results	15
Discussion	16
Conclusions	19
References	20
Figure Legends	25
Figures	26
Tables	35
Comprehensive Literature Review	36
1.0 Success Rate of Orthodontic Mini-Implants	36
2.0 OMI Failure	37
2.1 Cortical Bone	37
2.2 Stress and Strain	38
2.3 OMI Features	38
3.0 Implant Threads	41
4.0 Electronic Speckle Pattern Interferometry	43
5.0 Bone Analog Selection	45
6.0 Load Levels on OMIs	46
7.0 Bone-Implant Interface	47
8.0 Bone Strain and Resorption	48
References	49

Appendices

Appendix 1: Limitations	54
Appendix 2: Future Studies	56

LIST OF FIGURES

Figure	Page
1. Single-Thread (ST) and Dual-Thread (DT) OMIs.	27
2. Bone analog with cortical and cancellous components.	28
3. Placement of the 4 OMIs in each specimen block.	29
4. Optics table with mounted specimen block (a) and CCD camera (b).	30
5. Schematic diagram of electronic speckle pattern interferometer.	31
6. Setup of load apparatus on OMI.	32
7. Image captured by the CCD camera during testing.	33
8. Processed data allowing fringes to be visualized over time.	34
9. Specific strain versus distance from OMI.	35

LIST OF TABLES

Table	Page
1. Specifications of Single-Thread and Dual-Thread OMIs.	36
2. Physical properties of bone analog.	36
3. Specific strain ($\mu\epsilon/N$) at different increments from the OMI center.	36

Use of ESPI to evaluate the effect of thread design of orthodontic mini-implants on bone strain

Bryan J. Houlberg, DDS
Oregon Health and Science University
Department of Orthodontics
611 SW Campus Dr. SD 24
Portland, OR 97239
(310) 923-8742
houlberg@ohsu.edu

Todd Groesbeck, BS
Oregon Health and Science University
School of Dentistry
611 SW Campus Dr.
Portland, OR 97239
(801) 234-0158
groesbec@ohsu.edu

John C. Mitchell, PhD
Oregon Health and Science University
School of Dentistry
611 SW Campus Dr. SD 502
Portland, OR 97239
(503) 494-8977
mitchelj@ohsu.edu

Donald D. Duncan, PhD
Portland State University
Department of Electrical and Computer Engineering
1900 SW Fourth Ave. Suite 20-10
Portland, OR 97201
(503) 725-9044
duncadd1@cecs.pdx.edu

ABSTRACT

The purpose of this study was to measure the magnitude of bone strain imparted by orthodontic mini-implants (OMIs) of two different thread designs. OMIs with uniform thread pitch and diameter (Single-Thread, n=6) were compared against OMIs with two different thread pitches and diameters (Dual-Thread, n=6). The OMIs were inserted into bone analog, subjected to a ramped load from 0-30 N, and strain was detected and measured through electronic speckle pattern interferometry (ESPI). The ESPI method used a laser to project a speckle pattern of light on the bone analog, and as the analog was strained during OMI loading, fringes were produced in the speckle pattern that were detected by a camera and analyzed with custom software to quantify the amount of strain. Specific strain was measured at 1-mm intervals from the OMI center for each OMI. At 2 mm, significantly less ($p < 0.05$) specific strain was observed with Dual-Thread ($21.91 \mu\epsilon/N$) than with Single-Thread ($33.59 \mu\epsilon/N$). At 3 mm, the difference in specific strain between Dual-Thread ($15.75 \mu\epsilon/N$) and Single-Thread ($23.01 \mu\epsilon/N$) was highly significant ($p = 0.001$). At distances greater than 3 mm, no statistically significant difference in strain was observed between the two OMI types. This study demonstrated that OMIs with larger diameter and finer-pitch threads in the cortical bone region result in less strain in the bone immediately adjacent to the implants.

1 INTRODUCTION

The use of orthodontic mini-implants (OMIs) has gained popularity among orthodontists over the last decade due to their ability to provide anchorage without patient compliance or unwanted dental side effects. The success rate of these OMIs, as defined by their ability to remain stable throughout the period of time they are in use, has not been ideal. Recent clinical studies have reported their success rate to be only 80-90% [1-3].

OMI failure is due to a variety of factors related to the surrounding bone and properties of the OMIs themselves. Cortical bone thickness is significantly correlated with OMI stability [1, 4, 5], and studies on endosseous implants have shown that most implant failures can be attributed to excessive stresses and strains at the bone-implant interface [6, 7]. Studies examining how properties of OMIs influence their success have shown that geometric shape can impact stability and resistance to failure [8-11], length has little to no influence on success [2, 12, 13], and studies on diameter have had mixed results [2, 8, 12, 14-18].

Few studies have examined how thread design impacts the success rate of OMIs. In endosseous implants, Steigenga et al found that thread shape influences bone strain [19] and Kong et al showed that thread height and width impacts stress imparted to the bone [20]. Xu et al examined threads of osseointegrated implants used for prosthetic limbs and found that doubling the thread pitch significantly reduces the stress to the bone [21]. In two OMI studies, the diameter, pitch, and design of OMI threads were correlated with their stability [8, 10], but no investigation was made into how the thread design impacts the surrounding bone.

Currently there is a lack of research examining the effect of OMI thread design on bone strain. Electronic speckle pattern interferometry (ESPI) offers a non-contact method of analyzing surface displacements that are associated with strain [22]. In ESPI, a laser beam is projected onto a test object to create a speckle pattern of light. As the object is deformed, video

processing captures correlation fringes produced in the speckle pattern. These fringes can be analyzed to measure the amount of deformation, or strain, the object experienced during testing. Depending on the illumination strategy, viewing direction, and computer processing of the resulting data, ESPI is capable of measuring vibration, rigid body motion, and in-plane or out-of-plane deformations or strains [22]. ESPI has been used previously in dental research to examine physical properties of teeth and restorative materials [23-26]. ESPI has also been used to evaluate how the surface of bone deforms when loaded [27].

The purpose of this investigation was to measure the magnitude of bone strain imparted by OMIs of two different thread designs. Our hypothesis was that OMIs with threads of greater diameter and finer pitch in the cortical bone region would cause less strain in the surrounding bone, which could ultimately improve their clinical success rate.

2 MATERIALS AND METHODS

2.1 OMI Selection

OMIs (n=12) from Orthodontic TAADS (Memphis, TN) measured 7 mm in thread length and 1.0 mm in core diameter (Table 1). Six of the OMIs, designated “Single-Thread,” had a uniform thread pitch and diameter along its entire length, while another six, designated “Dual-Thread,” had two thread diameters and pitches (Fig 1). The secondary threads of the Dual-Thread OMIs were designed with a double-lead thread, thus having two starting points. This feature allowed the secondary threads to advance at the same rate as the primary threads, despite having twice the pitch, with the goal of preventing tearing of bone during insertion.

2.2 Specimen Preparation

The OMIs were inserted into a bone analog material (SAWBONES, Pacific Research Laboratories Inc, Vashon Island, WA) consisting of two components (Fig 2). The analog’s superficial layer was made of E-glass-filled epoxy sheets with a similar density [28- 30] and compressive modulus [31, 32] to cortical bone. This layer measured 1.5 mm in thickness to replicate the dimension of buccal cortical bone in the posterior maxilla or mandible [33, 34]. A deeper layer of the analog was made of solid rigid polyurethane foam with a similar density [35, 36] and compressive modulus [35, 37] to cancellous bone. The physical properties of these components are listed in Table 2. The bone analogs were sectioned into three pieces measuring 120 mm (L) x 50 mm (W) x 13 mm (D).

Specimen blocks were created by placing four OMIs in each section of bone analog as shown in Figure 3. The OMIs were placed in two rows, 40 mm from the ends of the analog and from each other, with the rows spaced 16.7 mm from the sides of the analog and from each other

to avoid overlapping strains during testing. Each of the specimen blocks contained two Single-Thread and two Dual-Thread OMIs. They were placed with the manufacturer's driver (Orthodontic TAADS, Memphis, TN) held in a hand-turned drill press (Shop-Task, Model 1720 XM Gold Series, USA), to ensure perpendicularity to the bone analog surface, until they were 1 mm from fully seated. Each OMI was then fully inserted by hand to a maximum insertion torque (MIT) of $25 \text{ Ncm} \pm 1 \text{ Ncm}$ as measured by a digital torque gauge. This torque value was obtained once the collar was in contact with the bone analog surface.

To rigidly hold the specimens and isolate deformation to the area around the OMI during load testing, each specimen block was inserted into a custom steel mounting base and embedded in Microstone (Whip Mix Corporation, Louisville, KY) to the analog's cortical bone-cancellous bone junction. The specimens were covered with a thin coat of flat silver spray paint (Rust-Oleum, Vernon Hills, IL) to facilitate visualization during testing. Each mounting base was rigidly fixed to an optics table so that the surface of the bone was perpendicular to the imaging axis of a Charged Couple Device (CCD) camera (Pt Grey GRAS-20S4M-C 1394b Grasshopper), as shown in Figure 4.

2.3 Testing

ESPI was used to measure the strain in bone. A diagram of the dual-beam ESPI configuration is shown in Figure 5. A Helium-Neon laser (Melles Griot, 25-LHP-928-249, Carlsbad, CA) was used as the light source and the CCD camera was the detector. The laser beam was split and the two beams simultaneously illuminated the OMI at angles of $\pm 11^\circ$ with respect to the surface normal of the bone analog. The OMIs were positioned in the center of the illumination pattern where the beams converged at a consistent height of 12.1 mm from the table

and 59 cm from the beam splitter. With this illumination pattern, the deformation fringes produced corresponded to displacements in the plane of loading of $\lambda/(2 \sin \alpha)$, where α is 11° and λ is the laser wavelength ($0.6328 \mu\text{m}$).

Each OMI was loaded by placing a 0.016 inch nickel ligature loop around each implant head and attaching it to a 50 lb load cell (Interface, Model MB-50, Scottsdale, AZ) mounted to a motorized stage. A ramped load from 0-30 N was applied perpendicular to the OMI and parallel to the bone analog surface (Fig 6). As the OMIs were loaded, deformation fringes in the speckle pattern were observed through the CCD camera that interfaced to a computer. Closely spaced fringes indicated higher displacement and more strain. These fringes were recorded with a custom LabView program (National Instruments, LabView for Windows 2000/XP version 8.2, Austin, TX) designed to continuously collect and analyze images from the CCD camera.

2.4 Statistical Analysis

LabView used digital image subtraction to analyze the strain in the bone analog. As the OMIs were loaded, each image captured by the camera was subtracted from the unloaded reference image, and the absolute value of this difference was formed and averaged along a continuum of distances from the OMI center. In this manner, a single trace of the compression-side specific strain ($\mu\epsilon/\text{N}$) was formed for each loaded OMI. The slope of the specific strain versus distance from the OMI was also calculated. Specific strain and slope values were compared with students t-test for differences with $\alpha = 0.05$.

3 RESULTS

One of the Dual-Thread OMIs was lost during testing. Results are therefore based on $n=6$ for Single-Thread and $n=5$ for Dual-Thread.

During testing of all OMIs, fringes in the speckle pattern moved tangentially away from the OMI in a circular pattern. As higher loads were applied, the fringes were more closely packed and began appearing at shorter intervals. Figure 7 shows a single frame captured by the camera during testing and Figure 8 shows the processed fringe data in LabView.

Strain was measured starting as close as possible to the OMI out to 6 mm from the OMI center. Strain values were converted to specific strain and were analyzed at 1-mm intervals, providing an average strain experienced along the load continuum at each interval (Table 3). At 2 mm, significantly less ($p < 0.05$) specific strain was observed with Dual-Thread ($21.91 \mu\epsilon/N$) than with Single-Thread ($33.59 \mu\epsilon/N$). At 3 mm, the difference in specific strain between Dual-Thread ($15.75 \mu\epsilon/N$) and Single-Thread ($23.01 \mu\epsilon/N$) was highly significant ($p = 0.001$). At distances of 4 mm and greater, no significant differences were observed.

Figure 9 shows the average specific strain for Single-Thread and Dual-Thread at varying distances from the OMI center. The slope of the specific strain versus distance from the OMI was calculated and compared between groups. The average slope for Single-Thread was steeper than the slope for Dual-Thread, but this difference was not significant ($p = 0.17$).

4 DISCUSSION

This study offers the first report of a research design that measured bone strain during OMI loading with a non-contact method. The ESPI method additionally offered the advantage of measuring strain along a continuum from the OMI, not just in the immediate proximity. While strain was measured on the compressive side in this study, ESPI also provides the advantage of potentially measuring strain at any direction around the OMI.

During testing, all OMIs were loaded from 0-30 N, which equates to approximately 0-3000 g. This amount of loading is a greater than what is typically applied clinically, as orthodontic forces applied to OMIs are in the range of 50-600 g [38-42]. The level of loading applied was selected because high loads produced multiple fringes, which were easily discernible in the images captured by the camera. However, at the lowest loads, only fractions of a single fringe were produced, and they were not discernible in the images captured by the camera. As a result, specific strain was used because it allowed for average strain values to be generated across the continuum of loads as a function of distance from the OMI.

This study found that within 3 mm of the implants, Dual-Thread OMIs produce less strain in bone upon loading than did Single-Thread OMIs. The lower strain values are most likely due to a greater surface area of thread being in contact with bone. Since stress and strain are proportional, imparting the same force over a larger area functionally reduces the stress at the bone-implant interface and the resulting bone strain. These findings agree with Xu et al who found that increasing thread diameter in surgical anchor implants reduced stress up to 40% in bone and 50% in the implant, making the stress distribution in the bone-implant contact area more uniform and moving maximal stresses away from the first implant thread [21]. In addition, Xu found that increasing thread pitch significantly reduced maximal stress [21]. In a finite element study on endosseous implants, Kong et al found that the highest stresses in bone were

concentrated in the cortical bone around the implant, and that these stresses increased as thread diameter decreased [20].

A greater bone-implant contact area has been related to reduced stress and strain in other studies. In a finite element study, Ding et al found that implants with a greater diameter, and therefore a greater bone-implant contact area, significantly reduced maximum stress and strain values [43]. As the diameter was increased by an average of 20%, the maximum stress was reduced by an average of 32% and the strain in bone was reduced by an average of 15%. Chou et al also examined endosseous implants in a finite element study [44]. He found that as the insertion depth of the implant was increased, effectively increasing the amount of bone in contact with the implant, that strain levels in the surrounding bone were significantly reduced.

Other studies have correlated the greater contact area at the bone-implant interface provided by OMIs with larger diameter and finer pitch threads with greater implant stability. Both Kim et al and Steigenga et al found that thread designs that allow for more contact at the bone-implant interface required more torque force to remove [10, 19]. Kim et al equated this greater removal torque with greater mechanical stability [10]. Steigenga et al reported that implants with threads in greater number and diameter provide more functional surface area, thus improving initial stability [19].

The lower strain values found with Dual-Thread OMIs could potentially result in less resorption at the bone-implant interface. Strain values were measured as close as possible to the bone analog-implant interface, although the OMI collar prevented measurement at the interface. When specific strain values are extrapolated to approximately the bone analog-implant interface, they equaled $28.1 \mu\epsilon/N (\pm 11.5)$ for Dual-Thread and $44.2 \mu\epsilon/N (\pm 11.4)$ for Single-Thread, which is significant at $p < 0.05$.

While the difference in specific strain between Dual-Thread and Single-Thread OMIs is statistically significant, the question arises whether this difference is clinically significant. Past studies have shown that between strains of 50-1500 $\mu\epsilon$ bone is in a healthy state of equilibrium, in the mild overload zone of 1500-3000 $\mu\epsilon$ bone undergoes anabolic modeling, and in the pathologic overload zone over 3000 $\mu\epsilon$ bone undergoes resorption [45, 46]. At orthodontic loads of 50-1000 g and using extrapolated strain values, strain generated at the bone analog-implant interface in this study ranged from 14-281 $\mu\epsilon$ for Dual-Thread and from 22-442 $\mu\epsilon$ for Single-Thread, both well below the pathologic overload threshold of 3000 $\mu\epsilon$. However, since bone is constantly being strained to some degree during functional loading, it is possible that the additional strain exerted by these loaded mini-implants could lead to bone resorption.

The slope of specific strain versus distance from OMI center for Single-Thread was steeper than for Dual-Thread OMIs, but the difference was not significant ($p = 0.17$). Given the significant difference in specific strain between the two OMI types, and the small sample size, a larger sample size would likely yield a statistically significant difference in slope. This result would mean that Single-Thread OMIs strain bone at a faster rate per unit load than Dual-Thread OMIs, which would explain the greater specific strain values at each distance for Single-Thread in this study.

5 CONCLUSION

The ESPI technique used in this study proved to be a valuable method of measuring and analyzing bone strain. This study demonstrated that during loading, OMIs with larger diameter and finer-pitch threads in the cortical bone region result in less strain in the surrounding bone immediately adjacent to the implants. This reduced strain in bone may result in less bone resorption due to excessive bone strain and thus fewer OMI failures.

REFERENCES

1. Motoyoshi M, Yoshida T, Ono A, Shimizu N. Effect of cortical bone thickness and implant placement torque on stability of orthodontic mini-implants. *Int J Oral Maxillofac Implants.* 2007;22:779-84
2. Wu TY, Kuang SH, Wu CH. Factors associated with the stability of mini-implants for orthodontic anchorage: a study of 414 samples in Taiwan. *J Oral Maxillofac Surg.* 2009;67:1595-9
3. Lim HJ, Eun CS, Cho JH, Lee KH, Hwang HS. Factors associated with initial stability of miniscrews for orthodontic treatment. *Am J Orthod Dentofacial Orthop.* 2009;136:236-42
4. Stahl E, Keilig L, Abdelgader I, Jäger A, Bourauel C. Numerical analyses of biomechanical behavior of various orthodontic anchorage implants. *J Orofac Orthop.* 2009;70:115-27
5. Huja SS, Litsky AS, Beck FM, Johnson KA, Larsen PE. Pull-out strength of monocortical screws placed in the maxillae and mandibles of dogs. *Am J Orthod Dentofacial Orthop.* 2005;127:307-313
6. Geng JP, Tan KB, Liu GR. Application of finite element analysis in implant dentistry: a review of the literature. *J Prosthet Dent.* 2001;85:585-98
7. Adell R, Lekholm U, Rockler B, Branemark P. A 15-year study of osseointegrated implants in the treatment of the edentulous jaw. *Int J Oral Surg.* 1981;10:387-416
8. Wilmes B, Ottenstreuer S, Su YY, Drescher D. Impact of implant design on primary stability of orthodontic mini-implants. *J Orofac Orthop.* 2008;69:42-50
9. Kim JW, Baek SH, Kim TW, Chang YI. Comparison of stability between cylindrical and conical type mini-implants: Mechanical and histological properties. *Angle Orthod.* 2008;78:692-8

10. Kim YK, Kim YJ, Yun PY, Kim JW. Effects of the taper shape, dual-thread, and length on the mechanical properties of mini-implants. *Angle Orthod.* 2009;79:908-14
11. Mischkowski RA, Kneuert P, Florvaag B, Lazar F, Koebke J, Zöllner JE. Biomechanical comparison of four different miniscrew types for skeletal anchorage in the mandibulo-maxillary area. *Int J Oral Maxillofac Surg.* 2008;37:948-54. Epub 2008 Sep 6
12. Miyawaki S, Koyama I, Inoue M, Mishima K, Sugahara T, Takano-Yamamoto T. Factors associated with the stability of titanium screws placed in the posterior region for orthodontic anchorage. *Am J Orthod Dentofacial Orthop.* 2003;124:373-8
13. Mortensen MG, Buschang PH, Oliver DR, Kyung HM, Behrents RG. Stability of immediately loaded 3- and 6-mm miniscrew implants in beagle dogs--a pilot study. *Am J Orthod Dentofacial Orthop.* 2009;136:251-9
14. Morarend C, Qian F, Marshall SD, Southard KA, Grosland NM, Morgan TA, McManus M, Southard TE. Effect of screw diameter on orthodontic skeletal anchorage. *Am J Orthod Dentofacial Orthop.* 2009;136:224-9
15. Wiechmann D, Meyer U, Büchter A. Success rate of mini- and micro-implants used for orthodontic anchorage: a prospective clinical study. *Clin Oral Implants Res.* 2007;18:263-7
16. Chen Y, Kyung HM, Zhao WT, Yu WJ. Critical factors for the success of orthodontic mini-implants: A systematic review. *Am J Orthod Dentofacial Orthop.* 2009;135:284-91
17. Kuroda S, Sugawara Y, Deguchi T, Kyung HM, Takano-Yamamoto T. Clinical use of miniscrew implants as orthodontic anchorage: success rates and postoperative discomfort. *Am J Orthod Dentofacial Orthop.* 2007;131:9-15

18. Park HS, Lee SK, Kwon OW. Group distal movement of teeth using microscrew implant anchorage. *Angle Orthod.* 2005;75:602-9
19. Steigenga JT, al-Shammari KF, Nociti FH, Misch CE, Wang HL. Dental implant design and its relationship to long-term implant success. *Implant Dent.* 2003;12:306-17
20. Kong L, Hu K, Li D, Song Y, Yang J, Wu Z, Liu B. Evaluation of the cylinder implant thread height and width: a 3-dimensional finite element analysis. *Int J Oral Maxillofac Implants.* 2008;23:65-74
21. Xu W, Crocombe AD, Hughes SC. Finite element analysis of bone stress and strain around a distal osseointegrated implant for prosthetic limb attachment. *Proc Inst Mech Eng H.* 2000;214:595-602
22. Jones R, Wykes C. *Holographic and Speckle Interferometry.* 2nd ed. Cambridge University Press; 1989
23. Bouillaguet S, Gamba J, Forchelet J, Krejci I, Wataha JC. Dynamics of composite polymerization mediates the development of cuspal strain. *Dent Mater.* 2006;22:896-902. Epub 2005 Dec 20
24. Zaslansky P, Friesem AA, Weiner S. Structure and mechanical properties of the soft zone separating bulk dentin and enamel in crowns of human teeth: insight into tooth function. *J Struct Biol.* 2006;153:188-99. Epub 2005 Dec 9
25. Kishen A, Kumar GV, Chen NN. Stress-strain response in human dentine: rethinking fracture predilection in postcore restored teeth. *Dent Traumatol.* 2004;20:90-100
26. Yap AU, Tan AC, Quan C. Non-destructive characterization of resin-based filling materials using Electronic Speckle Pattern Interferometry. *Dent Mater.* 2004;20:377-82

27. Shahar R, Weiner S. Insights into whole bone and tooth function using optical metrology. *J Mater Sci.* 2007;42:8919-33
28. Lees S, Heeley JD. Density of a sample bovine cortical bone matrix and its solid constituent in various media. *Calcif Tissue Int.* 1981;33:499-504
29. Cowin SC. *Bone Mechanics Handbook*. 2nd ed. Informa Healthcare; 2001
30. Blanton PL, Biggs NL. Density of fresh and embalmed human compact and cancellous bone. *Am J Phys Anthropol.* 1968;29:39-44
31. Martin RB, Burr DB, Sharkey NA. *Skeletal Tissue Mechanics*. Springer; 1998
32. Reilly DT, Burstein AH, Frankel VH. The elastic modulus for bone. *J Biomech.* 1974;7:271-5
33. Ono A, Motoyoshi M, Shimizu N. Cortical bone thickness in the buccal posterior region for orthodontic mini-implants. *Int J Oral Maxillofac Surg.* 2008;37:334-40
34. Baumgaertel S, Hans MG. Buccal cortical bone thickness for mini-implant placement. *Am J Orthod Dentofacial Orthop.* 2009;136:230-36
35. O'Mahony AM, Williams JL, Katz JO, Spencer P. Anisotropic elastic properties of cancellous bone from a human edentulous mandible. *Clin Oral Implants Res.* 2000;11:415-21
36. Johanson NA, Charlson ME, Cutignola L, Neves M, DiCarlo EF, Bullough PG. Femoral neck bone density. Direct measurement and histomorphometric validation. *J Arthroplasty.* 1993;8:641-52
37. Ravaglioli A, Krajewski A. *Bioceramics*. London: Chapman and Hall; 1992
38. Fritz U, Diedrich P, Kinzinger G, Al-Said M. The anchorage quality of mini-implants towards translatory and extrusive forces. *J Orofac Orthop.* 2003;64:293-304

39. Owens SE, Buschang PH, Cope JB, Franco PF, Rossouw PE. Experimental evaluation of tooth movement in the beagle dog with the mini-screw implant for orthodontic anchorage. *Am J Orthod Dentofacial Orthop.* 2007;132:639–646
40. Carrillo R, Rossouw PE, Franco PF, Opperman LA, Buschang PH. Intrusion of multiradicular teeth and related root resorption with mini-screw implant anchorage: a radiographic evaluation. *Am J Orthod Dentofacial Orthop.* 2007;132:647–655
41. Proffit WR, Fields HW, Sarver DM. *Contemporary Orthodontics.* 4th ed. Mosby Elsevier; 2007
42. Sung SJ, Jang GW, Chun YS, Moon YS. Effective en-masse retraction design with orthodontic mini-implant anchorage: a finite element analysis. *Am J Orthod Dentofacial Orthop.* 2010;137:648-57
43. Ding X, Zhu XH, Liao SH, Zhang XH, Chen H. Implant-bone interface stress distribution in immediately loaded implants of different diameters: A three-dimensional finite element analysis. *J Prosthodont.* 2009;18:393-402
44. Chou HY, Muftu S, Bozkaya D. Combined effects of implant insertion depth and alveolar bone quality on periimplant bone strain induced by a wide-diameter, short implant and a narrow-diameter, long implant. *J Prosthet Dent.* 2010;104:293-300
45. Frost HM. Skeletal structural adaptations to mechanical usage (SATMU): 1. Redefining Wolff's law: the bone modeling problem. *Anat Rec.* 1990;226:403-13
46. Frost HM. Wolff's law and bone's structural adaptations to mechanical usage: an overview for clinician's. *Angle Orthod.* 1994;64:175-88

FIGURE CAPTIONS

Fig. 1 Single-Thread (ST) and Dual-Thread (DT) OMIs.

Fig. 2 Photograph of bone analog with cortical (1.5 mm) and cancellous (13.5 mm) components.

Fig. 3 Placement of the 4 OMIs in each specimen block.

Fig. 4 Optics table with mounted specimen block (a) and CCD camera (b).

Fig. 5 Schematic diagram of electronic speckle pattern interferometer. Laser beam starts from the source (a), is directed through a beam splitter (b) and a series of mirrors (c), and is aimed precisely on the object with two spatial filters (d). Images of the illuminated object (e) are captured on the CCD camera (f).

Fig. 6 Load cell (a), ligature loop (b), specimen block (c), illumination pattern (d).

Fig. 7 Image captured by the CCD camera during testing. The dark rings are the displacement fringes produced during loading.

Fig. 8 Processed data allowing fringes to be visualized over time. Time zero is at the top of the image and proceeds downward. The OMI head is at the red bar in the center. The light blue curves correspond to fringes. The region between the black bars is selected for subsequent analysis.

Fig. 9 Specific strain versus distance from OMI.

Fig. 1



Fig. 2

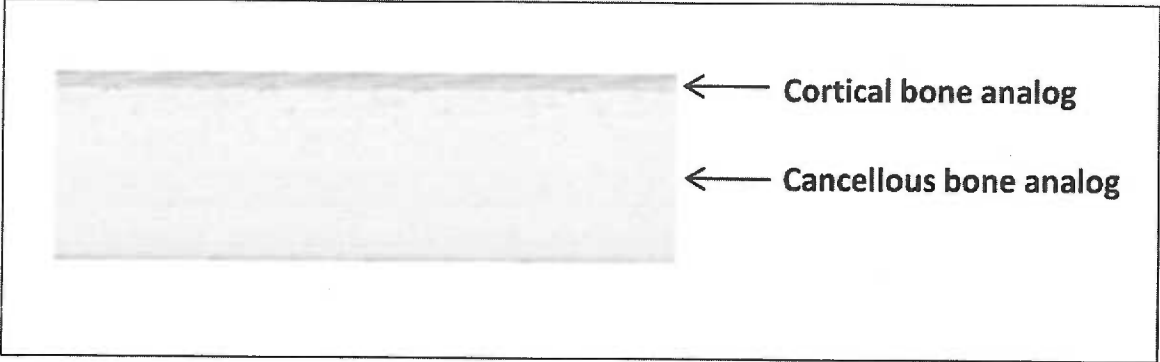


Fig. 3

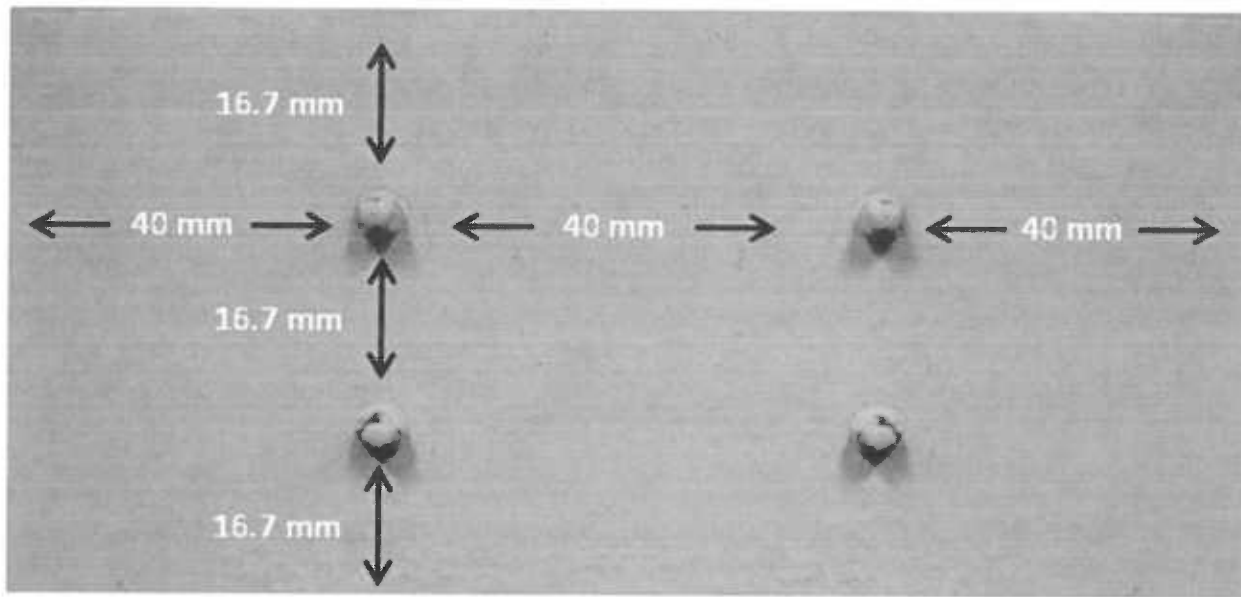


Fig. 4

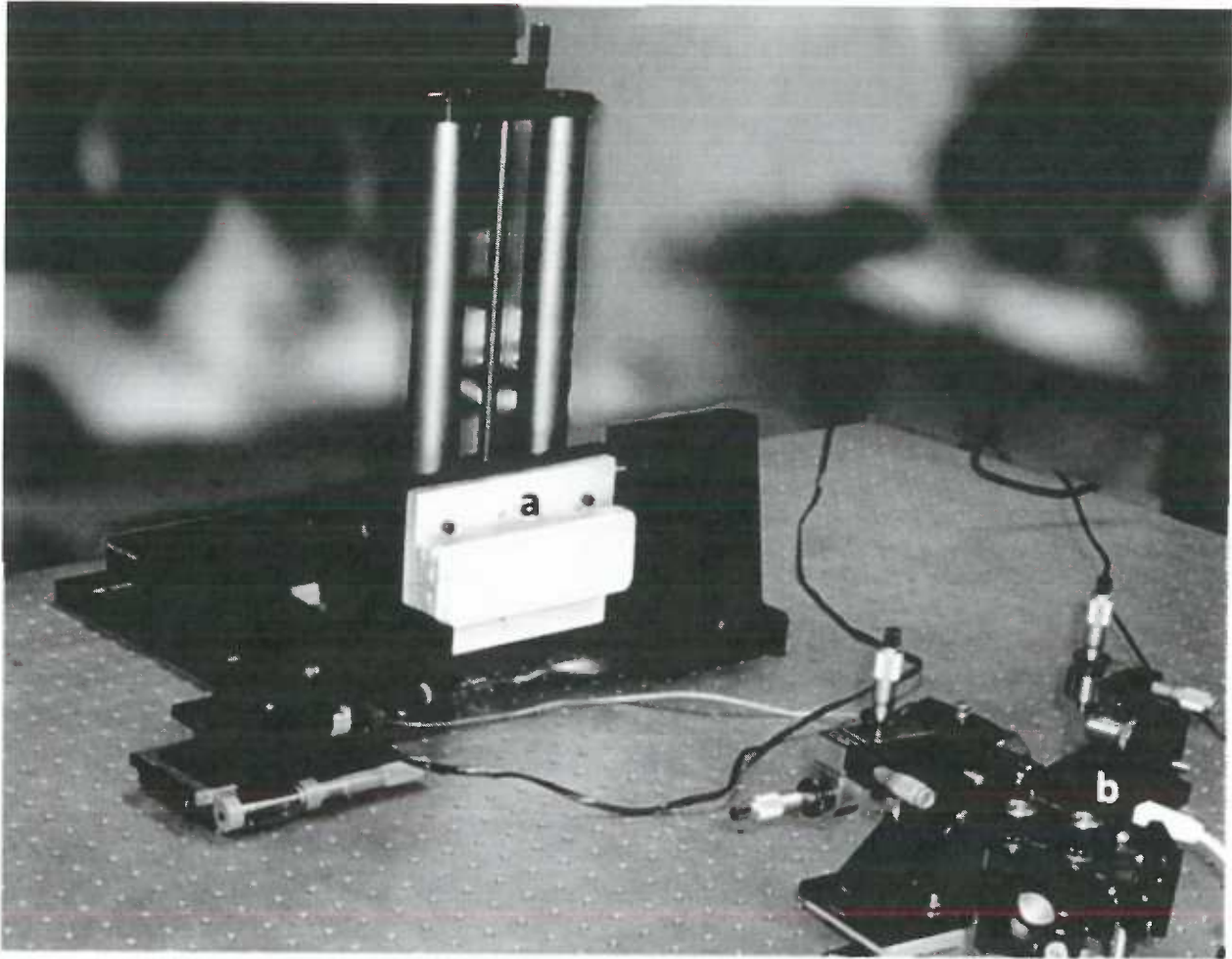


Fig. 5

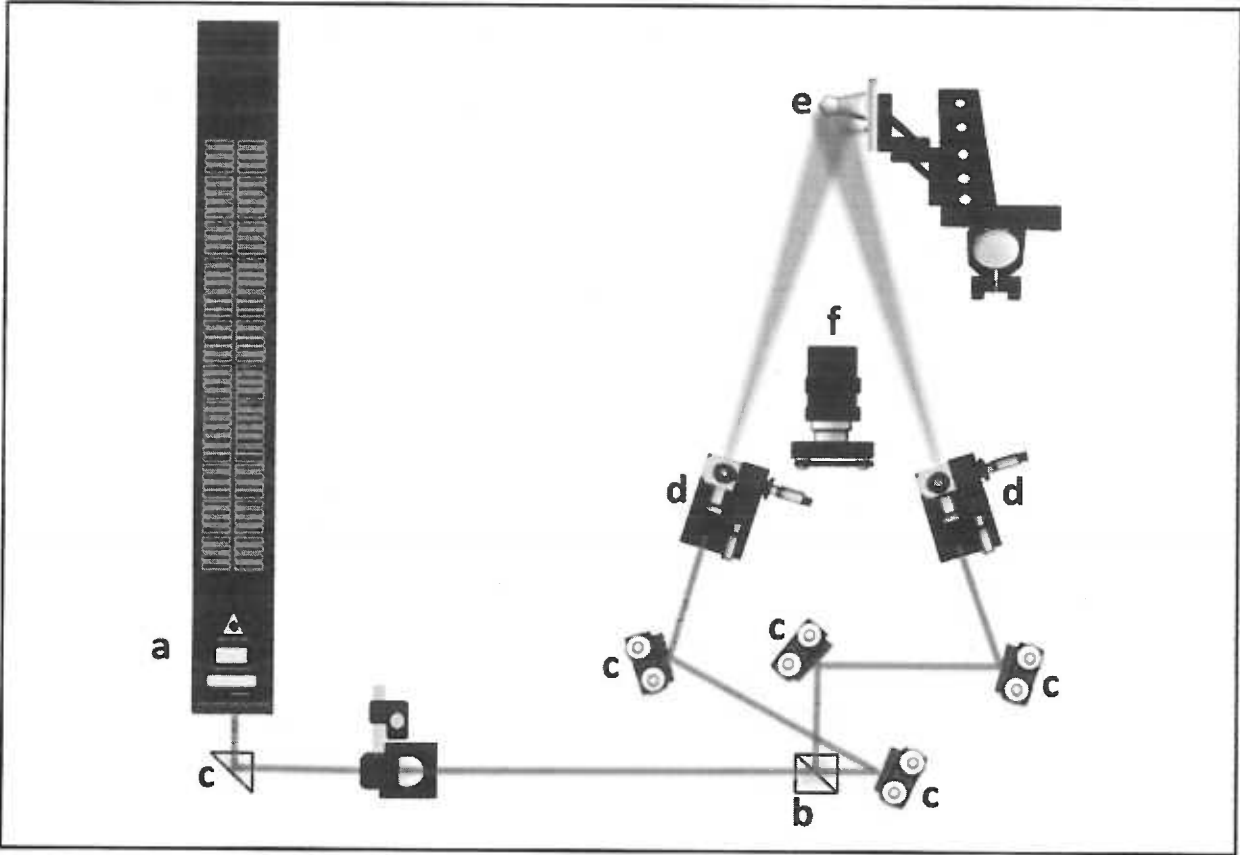


Fig. 6

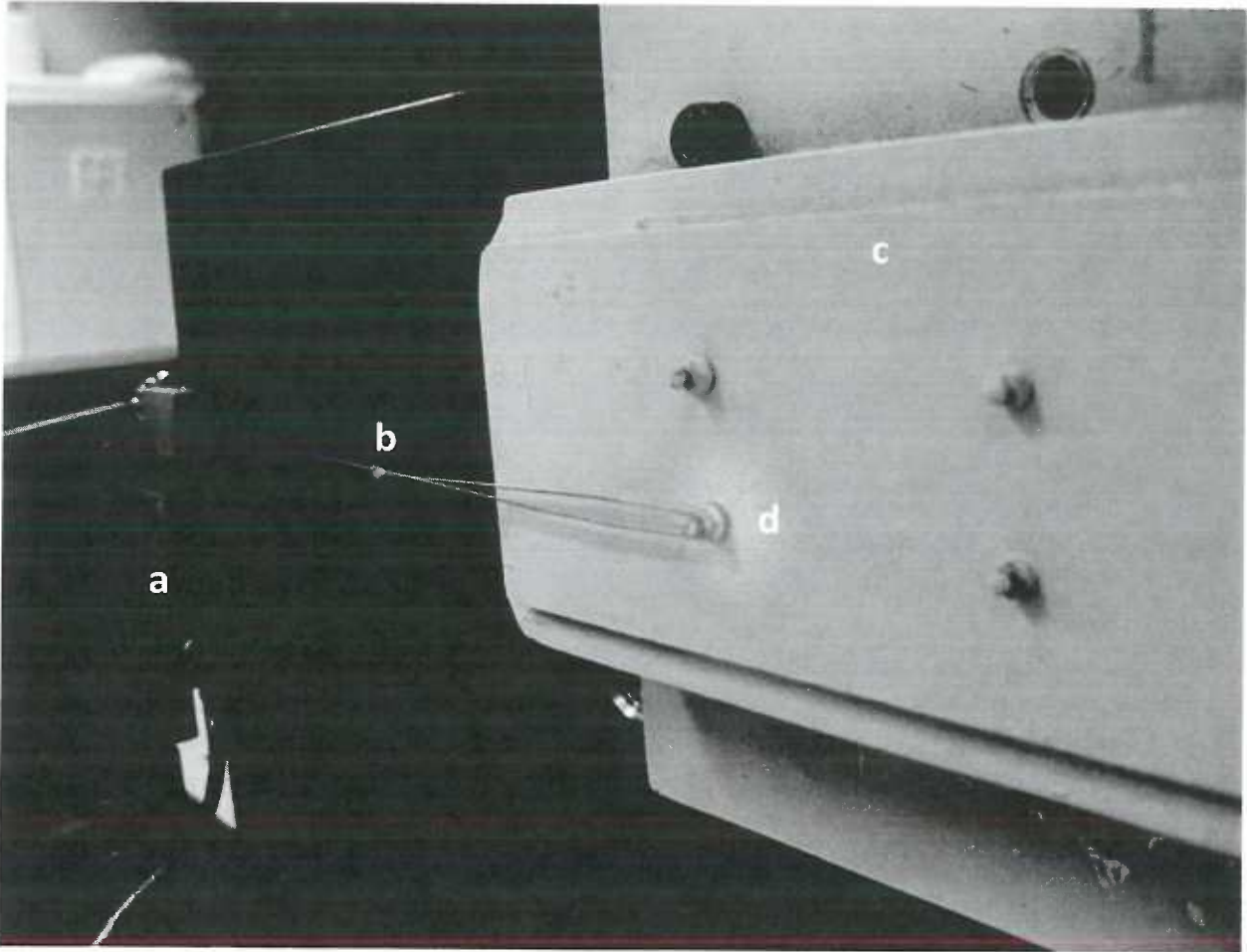


Fig. 7

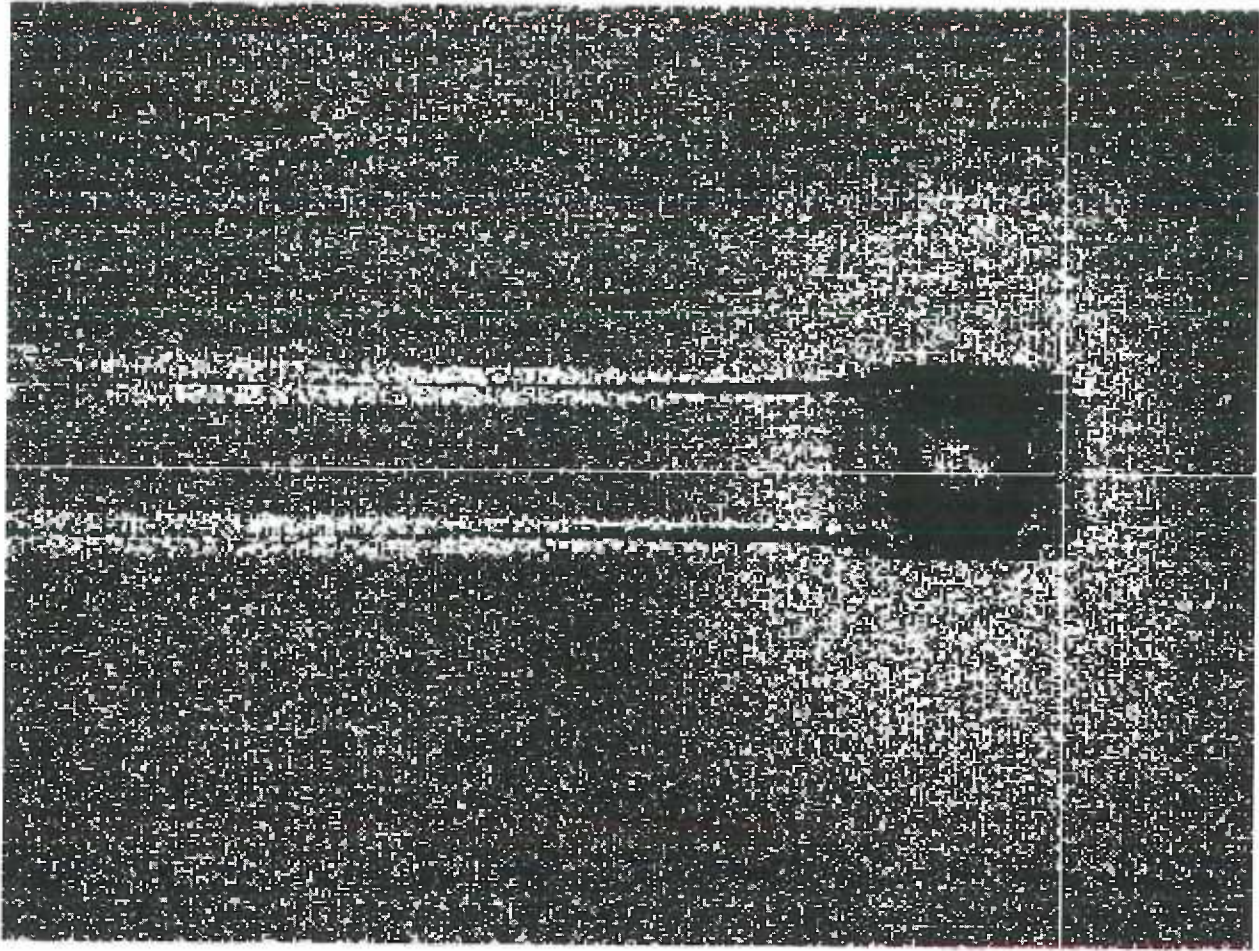


Fig. 8

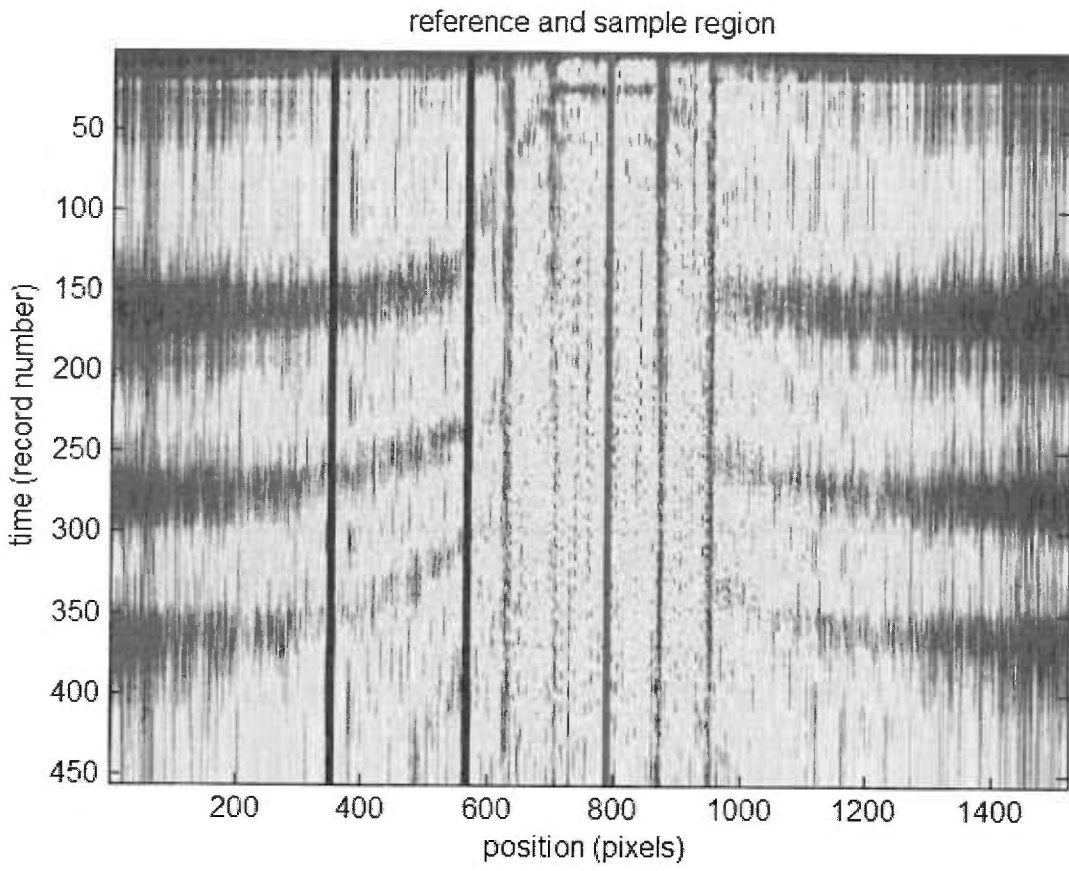


Fig. 9

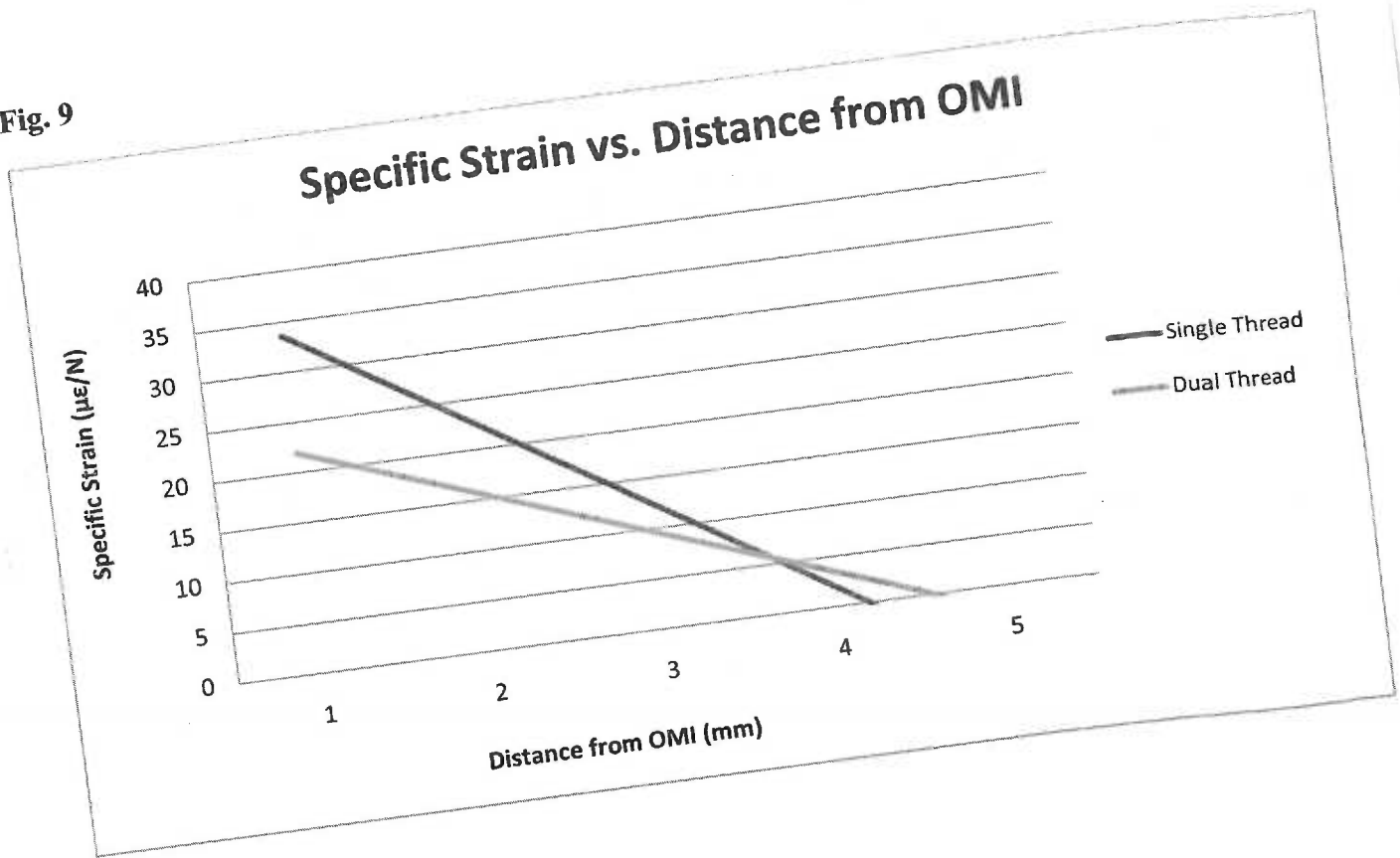


Table 1. Specifications of Single-Thread and Dual-Thread OMI.

OMI	Body Diameter (mm)	Thread 1 Diameter (mm)	Thread 2 Diameter (mm)	Thread 1 Pitch (threads/mm)	Thread 2 Pitch (threads/mm)	Thread 1 Length (mm)	Thread 2 Length (mm)
Single-Thread	1	1.5	-	1.6	-	7	-
Dual-Thread	1	1.5	2	1.6	3.2	5	2

Table 2. Physical properties of bone analog.

Bone Analog	Thickness (mm)	Density (g/cc)	Compressive Modulus (GPa)
Cortical Bone	1.5	1.64	16.7
Cancellous Bone	13.5	0.24	123

Table 3. Specific strain ($\mu\epsilon/N$) at different distances from the OMI center.

OMI	2 mm	3 mm	4 mm	5 mm	6 mm
Single-Thread	33.6 (± 6.8)	23.0 (± 3.0)	12.4 (± 3.9)	1.9 (± 8.1)	-8.7 (± 12.6)
Dual-Thread	21.9* (± 6.5)	15.6** (± 1.8)	9.6 (± 4.1)	3.4 (± 9.1)	-2.7 (± 14.2)

* Significantly less than Single-Thread at $p < 0.05$.

** Significantly less than Single-Thread at $p = 0.001$

COMPREHENSIVE LITERATURE REVIEW

1.0 Success Rate of Orthodontic Mini-Implants

The use of orthodontic mini-implants (OMIs) has gained popularity among orthodontists over the last decade due to their ability to provide anchorage without patient compliance or unwanted dental side effects. The success rate of these OMIs, as defined by their ability to remain stable throughout the period of time they are in use, has not been ideal. In a clinical study, Motoyoshi et al examined the effect of cortical bone thickness, inter-root distance, distance from the alveolar crest to the bottom of the maxillary sinus at the prepared implant site, and implant placement torque on OMI success.¹ They placed 87 OMIs in 32 patients and found an overall success rate of 87%.

Wu et al also ran a clinical study on OMIs.² In his study, 414 OMIs were placed in 166 patients. He evaluated failure rates and factors associated with the stability of OMIs. They found a success rate of 89.9% and stated that most failures occurred within the first two weeks of OMI placement. They found no relationship between age or gender and OMI failure. In another clinical study, Lim et al investigated various factors associated with initial OMI stability.³ They associated initial stability with OMI success. In their study, 378 OMIs were placed in 154 patients and many variables were recorded and measured. In accordance with the previous two studies, Lim et al found a success rate of 83.6%, and he found no statistically significant association between age, sex, placement site, tissue mobility, or factors related to OMI parameters and OMI success.

2.0 OMI Failure

Many studies have looked into the factors related to OMI failure, and some of the most commonly examined factors are the cortical bone, stresses and strains at the bone-implant interface, and factors inherent in the OMIs themselves.

2.1 *Cortical Bone*

In the aforementioned clinical study by Motoyoshi et al, they measured cortical bone thickness in all 32 patients with computerized tomography imaging before OMI placement.¹ The study found that cortical bone thickness was significantly greater in the success group (1.42 ± 0.59 mm) than in the failure group (0.97 ± 0.31 mm). They also stated that the odds ratio for failure of the OMI was 6.93 when the cortical bone thickness was less than 1 mm compared to thicknesses greater than 1 mm.

Stahl et al examined the effect of various material parameters in regard to various OMI types, sizes, and load directions using the finite element method.⁴ They used simulated cortical bone thicknesses of 1 mm and 2mm and found that OMI deflections increased with a lower Young's modulus of cancellous bone for the 1 mm cortical bone thickness group, but not the 2 mm cortical bone thickness group. They concluded that when the cortical bone is thinner, OMI mobility becomes more dependent on cancellous bone, but stability is primarily related to cortical bone and only secondarily to cancellous bone.

Huja et al examined whether the pull-out strength of OMIs in bone varies depending on the site of insertion in the maxilla or mandible.⁵ They placed 56 OMIs in the anterior, middle, and posterior regions of the maxilla and mandible of beagle dogs and measured the pull-out strength and cortical bone thickness at each location. They found that the anterior mandible had

significantly lower pull-out strength than the posterior mandible and concluded that there was a significant correlation between pull-out strength and cortical bone thickness.

2.2 Stress and Strain

Excessive stresses and strains at the bone-implant interface have also been linked with OMI failure. In a systematic review, Geng et al reviewed the use of finite element analysis on endosseous implants in relation to the bone-implant interface, the implant-prosthesis connection, and multiple-implant prostheses.⁶ They concluded from his review, that with regard to endosseous implants, stress at the bone-implant interface is a major determinant of implant success since excessive stresses can lead to bone resorption at the bone-implant interface, which results in implant failure.

In 1980, Adell et al concluded a 15-year study in which they placed 2,768 endosseous implants into the jaws of 371 consecutive patients and analyzed success and failure.⁷ They attributed the 10-20% failure rate to improper osseointegration and cited excessive stresses at the bone-implant interface as a primary factor impeding proper osseointegration.

2.3 OMI Features

Multiple studies have examined how the features of OMIs themselves impact success and failure. In particular, OMI shape, length, and diameter have been investigated. Wilmes et al analyzed the impact of implant design and dimension on primary stability.⁸ They placed 6 different OMIs of varying lengths, diameters, and shapes into porcine iliac bone segments. They analyzed insertion torque, relating it to primary stability. They found that conical OMIs had

higher insertion torques, and therefore higher primary stabilities, than cylindrical-shaped OMI. They also found that a larger diameter OMI has a higher primary stability.

Kim et al investigated the mechanical and histological properties of conical and cylindrical shaped OMI.⁹ All OMIs were placed into Sawbones, insertion and removal torques were measured, and histomorphologic analysis was conducted afterward in beagle dogs. They found that the conical group showed significantly higher insertion torque and removal torque than the cylindrical group. These higher torque values for conical OMIs Kim et al equated with greater stability.

In a different study by Kim et al, the effects of length, cylindrical and taper shapes, and dual-thread on insertion and removal torques were analyzed.¹⁰ Similar to the previous study, all OMIs were placed in Sawbones. Again, cylindrical OMIs were shown to have the lowest insertion and removal torques, showing that conical shaped OMIs have a greater primary stability. The results of this study with regard to threads are discussed later in the literature review. Mischkowski et al compared 4 OMI types for skeletal anchorage regarding their biomechanical properties contributing to primary stability.¹¹ They measured insertion torque and pull-out strength in axial, 20-degree, and 40-degree insertions. They also found that conical OMIs had a higher insertion torque and concluded that they achieve higher primary stability compared to cylindrical OMIs.

Miyawaki et al examined the factors associated with the stability of OMIs placed in the buccal alveolar bone of the posterior region.¹² He looked at 134 OMIs of three different types and compared them with 17 bone plates. He found that OMIs with a 1 mm diameter had a significantly lower success rate than OMIs with a diameter of 1.5 mm or 2.3 mm. He further found no association with OMI length on success.

In another study looking at OMI length, Mortensen et al placed 3 mm and 6 mm OMIs in the jaws of beagle dogs, and immediately loaded them for 6 weeks.¹³ He used forces of 600 g in the maxilla and 600 or 900 g in the mandible. He found that the success rates of the 3 mm OMIs were significantly lower than for the 6 mm OMIs. This is one of the only studies that cite a significant difference in success with different OMI lengths, but it is also one of the only studies that examine OMIs as short as 3 mm. The aforementioned study by Wu et al examining failure rates and factors associated with the stability of OMIs also looked at length and diameter as potential factors.² In the maxilla, they found a lower failure rate for diameters less than or equal to 1.4 mm. With regard to length, they found no statistical difference between 10 mm and 13 mm lengths.

Morarend et al compared the force resistance of larger-diameter monocortical OMIs to smaller-diameter monocortical OMIs.¹⁴ They also compared the force resistance of larger-diameter monocortical OMIs to smaller-diameter bicortical OMIs. They placed all OMIs into hemisected maxillas and mandibles. They found that anchorage force values of 2.5 mm OMIs with monocortical anchorage were greater than 1.5 mm OMIs with monocortical anchorage, both in the maxilla and mandible. They found no difference between 2.5 mm monocortical and 1.5 mm bicortical OMIs in the mandible, but the 1.5 mm bicortical OMIs had greater anchorage force values than the 2.5 mm monocortical OMIs in the maxilla. They concluded that larger-diameter OMIs provide greater anchorage than smaller-diameter OMIs so long as they are monocortical. They further concluded that smaller-diameter bicortical OMIs provide at least as much anchorage as larger-diameter monocortical OMIs.

Wiechmann et al evaluated the success rates of OMIs with two different diameters, 1.1 and 1.6 mm.¹⁵ They placed 133 OMIs in the maxilla and mandible of patients and statistically

analyzed which diameter OMIs had a higher success rate. They found that significantly more 1.1 mm diameter OMIs failed than 1.6mm diameter OMIs, and they concluded that a larger diameter leads to greater stability.

In a systematic review on the factors for the success of OMIs, Chen et al looked at many different parameters of OMIs, including length and diameter.¹⁶ They found no association between OMI length and success in the literature. With regard to diameter, their findings were mixed. They cited multiple studies stating larger diameter OMIs have greater stability. However, they pointed to just as many studies that show OMIs with a smaller diameter have greater stability.

One such study which showed no effect of diameter on OMI stability was done by Kuroda et al.¹⁷ They placed 116 OMIs of two different diameters into 75 patients and examined their success rate. He found no statistical difference in stability between OMIs with a diameter of 1.3 mm and those with a diameter of 2.3 mm. Park et al also examined the success rates of OMIs with respect to diameter.¹⁸ They placed many micro-implants with a diameter of 1.3 mm and a few OMIs with a diameter of 2 mm. The study found the larger diameter OMIs had a higher failure rate than the micro-implants. However, this is one of the few studies reporting lower success with larger diameter. The sample size of the 2 mm OMIs was small in this study.

3.0 Implant Threads

There have been multiple studies evaluating how the threads of endosseous implants influence stress and strain at the bone-implant interface, and their clinical success rate. In one study, Steigenga et al reviewed the effects of the biomechanical aspects of dental implant design on the quality and strength of osseointegration, the bone-implant interface, and their relationships

to long-term success.¹⁹ The authors stated that threads function to maximize initial contact, improve initial stability, enlarge implant surface area, and favor dissipation of stress. In this review, they concluded that square thread shapes, which provide more bone-implant contact than V-shaped threads, have an optimized surface area for compressive load transmission resulting in a lower strain profile to bone.

Another study by Kong et al evaluated continuous variations of thread height and width for an experimental endosseous implant with the finite element analysis.²⁰ They examined only V-shaped threads, and varied the height from 0.2-0.6 mm and the width from 0.1-0.4 mm. They placed forces both along the axis of the implant and at a 45-degree angle. Kong et al found that stress in bone was more sensitive to thread height than width and that cancellous bone was more sensitive to change in thread parameters than was cortical bone. They found a thread height of 0.34-0.5 mm and a thread width of 0.18-0.3 mm were optimal for reducing stress within bone.

In another finite element study, Xu et al investigated the effect of varying surgical anchor length, diameter, and thread pitch on stress and strain distributions at the bone-implant interface.²¹ They found that increasing the external diameter of the implant will reduce the maximal stress in the interface area without increasing the stress significantly in the area of the implant shaft, thus decreasing the overall strains in the bone. They also found that changing the implant length had little effect on stress and strain. With regard to implant threads, they found that increasing thread diameter reduced stress up to 40% in bone and 50% in the implant, making the stress distribution in the bone-implant contact area more uniform and moving maximal stresses away from the first implant thread. In addition, Xu found that doubling thread pitch significantly reduced maximal stress at the bone-implant interface.

There have been only a couple studies that examined the effect of OMI threads on stability. In the aforementioned study by Wilmes et al, they looked at the insertion torque of multiple implant types, shapes, and parameters in porcine bone.⁸ They stated in their conclusions that the diameter and design of the OMI thread have a distinctive impact on primary stability, but never stated in what way or how they came to that conclusion. The previously mentioned study by Kim et al on dual-thread OMIs found that OMIs with a higher thread pitch in the cortical bone region had significantly higher insertion and removal torque.¹⁰ They equated these findings with greater mechanical stability than OMIs with a uniform thread pitch along its entire length.

4.0 Electronic Speckle Pattern Interferometry

Jones and Wykes wrote a book in 1989 describing how Electronic Speckle Pattern Interferometry (ESPI) is one of the most advanced optical methods of measuring displacement and strain with a non-contact technique.²² Instead of using a strain gauge attached to the test object, this process uses laser light, together with video detection, recording, and processing to visualize static and dynamic displacements of objects undergoing deformation. When the object is subjected to a load, correlation fringes are produced in the speckle pattern focused on the test object. These fringes are detected by a camera that interfaces with a computer. With custom software, these fringes can be analyzed to determine how much displacement and strain was present in the object when loaded.

Jones and Wykes went on to further explain how the software converts the correlation fringes to strain measurements.²² The software uses a process called digital image subtraction where images of the correlation fringes detected by the camera during loading are subtracted

from a reference image of the unloaded object already stored on the camera. In this way, strain measurements can be recorded at each unit of time and this information can be combined with the load history recorded at each unit of time to determine how much strain was present in the system for each unit of load.

ESPI has been used numerous times in dental research to measure physical properties of teeth and dental materials. Bouillaguet et al used ESPI to measure tooth deformation in response to polymerization of five resin composites with a range of polymerization shrinkage and found it to be a viable method of measuring cuspal strain.²³ Zaslansky et al found ESPI to be a reliable technique for measuring the deformation and stiffness of the zone of dentin beneath enamel.²⁴ Kishen et al found ESPI useful for measuring the in-plane and out-of-plane response of human dentin to thermal loads in real time.²⁵ Yap et al loaded resin-based materials and found ESPI a viable method of characterizing the modulus of these materials.²⁶

In 2007, Shahar et al reviewed optical metrology methods, including ESPI, for their effectiveness in examining material properties of complex structures like bone.²⁷ Shahar cited a few studies that used ESPI to evaluate deformation in bone including mice femur loading and sheep fracture healing. ESPI allowed those researchers to find different patterns of strain distribution depending on the load applied, and that the highest strains in loaded fractured bone occur in the fracture gap. Shahar concluded from these studies that ESPI makes it possible to not only study the mechanical behavior of entire structures like bone, but ESPI could also contribute significantly to our understanding of questions regarding structure-function relations in bone.

5.0 Bone Analog Selection

Since bone quality and thickness are major determinants of mini-implant success,^{1,4,5} much care was given to the selection of bone analog in this study. Ono et al investigated the cortical bone thickness in the buccal posterior region mesial and distal to the first molar, where OMI's are often placed.³³ He used CT imaging from 1 to 15 mm below the alveolar crest at 1 mm intervals in 43 OMI patients. They found an average thickness of 1.09-2.21 mm in the maxilla and 1.59-3.03 mm thick in the mandible. Baumgaertel et al also investigated the buccal cortical bone thickness by taking CT images of 30 dry skulls with slices through every interdental area.³⁴ They found buccal cortical bone thickness was greater in the mandible (1.5-2.3 mm) than in the maxilla (1.0-1.3 mm). In connection with these two studies, a cortical bone analog of 1.5mm was chosen as a good average of cortical bone thicknesses in the maxilla and mandible.

The cortical bone analog used in our study had a density of 1.64 g/cc and a compressive modulus of 16.7 GPa, which is similar to cortical bone properties reported in other studies. Lees measured the density of bovine cortical bone to be 1.33 g/cc when wet and 1.42 g/cc when dried.²⁸ In his book on bone mechanics, Cowin listed the density of human cortical bone as high as 1.91 g/cc.²⁹ Blanton et al looked at the properties of fresh and embalmed bone and found the density fresh and embalmed cortical bone to both be 1.85 g/cc.³⁰ With regard to the compressive modulus of cortical bone, Martin et al and Reilly et al reported the modulus of human cortical bone to be 17.4 GPa and 17.9 GPa respectively.^{31,32}

The cancellous bone analog in our study had a density of 0.24 g/cc and a compressive modulus of 123 MPa, which also were both similar to cancellous bone properties reported by other authors. O'Mahony et al conducted a study in which he took seven samples of cancellous

bone from the edentulous mandible and measured their density and compressive modulus.³⁵ He found the density of cancellous bone averaged 0.55 g/cc and the modulus averaged 114 MPa. Johanson et al measured the density of cancellous bone in the human femoral neck and found that density ranged from 0.48-1.04 g/cc.³⁶ In a book on properties of cancellous bone, Ravaglioli et al reported the modulus of cancellous bone to be in the range of 90-230 MPa.³⁷

6.0 Load Levels on OMIs

The load levels applied to the OMIs in this study were in the range of 0-3000 g of force, which are much higher than load levels applied to OMIs in clinical situations. Many studies have been performed on dogs to determine appropriate force levels to apply to OMIs. In a study done on foxhounds, Fritz et al placed 16 OMIs into their jaws and applied forces between 50-200 cN, or approximately 50-200 g of force.³⁸ They found that all OMIs remained stable throughout the test period. Owens et al placed OMIs in the mouths of beagle dogs and applied a force of 25 g to half of them and 50 g to the other half.³⁹ They found no significant difference in success between the two different force levels. Carrillo et al also placed OMIs in the mouths of beagle dogs and applied a 50 g, 100 g, or 200 g force.⁴⁰ They found no significant difference in success rate with these force levels, and none of the force levels produced significant root resorption on the teeth being intruded.

There is also information published in the literature with regard to clinical force levels in human patients. Proffit has reported the ideal force to be applied to teeth for orthodontic movement to be in the range of 35-120 g per tooth.⁴¹ In situations where extraoral forces are being applied or skeletal movement is desired, forces can enter the range of 500-1000 g on each side of the jaw. Since forces applied to OMIs can be for orthodontic movement of a single tooth

or for skeletal movement, a force range of 35-500 g on a single OMI can be expected. A recent finite element study by Sung et al used similar force levels as they replicated a clinical situation of en-masse retraction of anterior teeth with OMIs. They used force levels between 50-200 g.⁴²

7.0 Bone-Implant Interface

Studies have shown that a greater surface area of implant in contact with bone results in less stress and strain at the bone-implant interface. Ding et al used a finite element model to analyze the stress distribution in bone around endosseous implants of different diameters.⁴³ Using diameters of 3.3 mm, 4.1 mm, and 4.8 mm and a force level of 150 N, Ding and colleagues found that implants with a greater diameter, and therefore a greater surface area of implant in contact with bone, significantly reduced maximum stress and strain values. Specifically, they found that as the diameter increased by an average of 20%, the maximum stress was reduced by an average of 32% and the strain in bone was reduced by an average of 15%.

Chou et al used a finite element method to evaluate the biomechanical response of the jaw bone to endosseous implants of varying lengths and diameters. They used implants with diameters of 3.5 mm and 5 mm and lengths of 6 mm and 10.7 mm, and applied a force of 100 N. Chou found that, regardless of the diameter, strain levels in peri-implant bone were reduced as the insertion depth, and therefore the surface area of implant in contact with bone, was increased.⁴⁴

8.0 Bone Strain and Resorption

Frost has been prolific in bone biology literature in explaining how bone responds to various levels of strain.^{45,46} According to Frost, when bone strain levels dip below 50 $\mu\epsilon$, the largest disuse effects on remodeling occur, and resorption is happening. At levels between 50-1500 $\mu\epsilon$, bone is in a healthy state of equilibrium with neither resorption or modeling outweighing the other. At levels between 1500-3000 $\mu\epsilon$, bone is in a mild overload zone and anabolic modeling is occurring. By adding to, reshaping, and strengthening bone, those modeling drifts reduce future strains under the same mechanical loads towards that strain region. Strains above 3000 $\mu\epsilon$ put bone in the pathologic overload zone and resorption outweighs modeling. Frost states that such strains also increase bone microdamage. At extreme levels of microstrain, above 25,000 $\mu\epsilon$, bone fractures.

LITERATURE REVIEW REFERENCES

1. Motoyoshi M, Yoshida T, Ono A, Shimizu N. Effect of cortical bone thickness and implant placement torque on stability of orthodontic mini-implants. *Int J Oral Maxillofac Implants.* 2007;22:779-84
2. Wu TY, Kuang SH, Wu CH. Factors associated with the stability of mini-implants for orthodontic anchorage: a study of 414 samples in Taiwan. *J Oral Maxillofac Surg.* 2009;67:1595-9
3. Lim HJ, Eun CS, Cho JH, Lee KH, Hwang HS. Factors associated with initial stability of miniscrews for orthodontic treatment. *Am J Orthod Dentofacial Orthop.* 2009;136:236-42
4. Stahl E, Keilig L, Abdelgader I, Jäger A, Bourauel C. Numerical analyses of biomechanical behavior of various orthodontic anchorage implants. *J Orofac Orthop.* 2009;70:115-27
5. Huja SS, Litsky AS, Beck FM, Johnson KA, Larsen PE. Pull-out strength of monocortical screws placed in the maxillae and mandibles of dogs. *Am J Orthod Dentofacial Orthop.* 2005;127:307-313
6. Geng JP, Tan KB, Liu GR. Application of finite element analysis in implant dentistry: a review of the literature. *J Prosthet Dent.* 2001;85:585-98
7. Adell R, Lekholm U, Rockler B, Branemark P. A 15-year study of osseointegrated implants in the treatment of the edentulous jaw. *Int J Oral Surg.* 1981;10:387-416
8. Wilmes B, Ottenstreuer S, Su YY, Drescher D. Impact of implant design on primary stability of orthodontic mini-implants. *J Orofac Orthop.* 2008;69:42-50
9. Kim JW, Baek SH, Kim TW, Chang YI. Comparison of stability between cylindrical and conical type mini-implants: Mechanical and histological properties. *Angle Orthod.* 2008;78:692-8

10. Kim YK, Kim YJ, Yun PY, Kim JW. Effects of the taper shape, dual-thread, and length on the mechanical properties of mini-implants. *Angle Orthod.* 2009;79:908-14
11. Mischkowski RA, Kneuert P, Florvaag B, Lazar F, Koebke J, Zöllner JE. Biomechanical comparison of four different miniscrew types for skeletal anchorage in the mandibulo-maxillary area. *Int J Oral Maxillofac Surg.* 2008;37:948-54. Epub 2008 Sep 6
12. Miyawaki S, Koyama I, Inoue M, Mishima K, Sugahara T, Takano-Yamamoto T. Factors associated with the stability of titanium screws placed in the posterior region for orthodontic anchorage. *Am J Orthod Dentofacial Orthop.* 2003;124:373-8
13. Mortensen MG, Buschang PH, Oliver DR, Kyung HM, Behrents RG. Stability of immediately loaded 3- and 6-mm miniscrew implants in beagle dogs--a pilot study. *Am J Orthod Dentofacial Orthop.* 2009;136:251-9
14. Morarend C, Qian F, Marshall SD, Southard KA, Grosland NM, Morgan TA, McManus M, Southard TE. Effect of screw diameter on orthodontic skeletal anchorage. *Am J Orthod Dentofacial Orthop.* 2009;136:224-9
15. Wiechmann D, Meyer U, Büchter A. Success rate of mini- and micro-implants used for orthodontic anchorage: a prospective clinical study. *Clin Oral Implants Res.* 2007;18:263-7
16. Chen Y, Kyung HM, Zhao WT, Yu WJ. Critical factors for the success of orthodontic mini-implants: A systematic review. *Am J Orthod Dentofacial Orthop.* 2009;135:284-91
17. Kuroda S, Sugawara Y, Deguchi T, Kyung HM, Takano-Yamamoto T. Clinical use of miniscrew implants as orthodontic anchorage: success rates and postoperative discomfort. *Am J Orthod Dentofacial Orthop.* 2007;131:9-15

18. Park HS, Lee SK, Kwon OW. Group distal movement of teeth using microscrew implant anchorage. *Angle Orthod.* 2005;75:602-9
19. Steigenga JT, al-Shammari KF, Nociti FH, Misch CE, Wang HL. Dental implant design and its relationship to long-term implant success. *Implant Dent.* 2003;12:306-17
20. Kong L, Hu K, Li D, Song Y, Yang J, Wu Z, Liu B. Evaluation of the cylinder implant thread height and width: a 3-dimensional finite element analysis. *Int J Oral Maxillofac Implants.* 2008;23:65-74
21. Xu W, Crocombe AD, Hughes SC. Finite element analysis of bone stress and strain around a distal osseointegrated implant for prosthetic limb attachment. *Proc Inst Mech Eng H.* 2000;214:595-602
22. Jones R, Wykes C. *Holographic and Speckle Interferometry.* 2nd ed. Cambridge University Press; 1989
23. Bouillaguet S, Gamba J, Forchelet J, Krejci I, Wataha JC. Dynamics of composite polymerization mediates the development of cuspal strain. *Dent Mater.* 2006;22:896-902. Epub 2005 Dec 20
24. Zaslansky P, Friesem AA, Weiner S. Structure and mechanical properties of the soft zone separating bulk dentin and enamel in crowns of human teeth: insight into tooth function. *J Struct Biol.* 2006;153:188-99. Epub 2005 Dec 9
25. Kishen A, Kumar GV, Chen NN. Stress-strain response in human dentine: rethinking fracture predilection in postcore restored teeth. *Dent Traumatol.* 2004;20:90-100
26. Yap AU, Tan AC, Quan C. Non-destructive characterization of resin-based filling materials using Electronic Speckle Pattern Interferometry. *Dent Mater.* 2004;20:377-82

27. Shahar R, Weiner S. Insights into whole bone and tooth function using optical metrology. *J Mater Sci.* 2007;42:8919-33
28. Lees S, Heeley JD. Density of a sample bovine cortical bone matrix and its solid constituent in various media. *Calcif Tissue Int.* 1981;33:499-504
29. Cowin SC. *Bone Mechanics Handbook.* 2nd ed. Informa Healthcare; 2001
30. Blanton PL, Biggs NL. Density of fresh and embalmed human compact and cancellous bone. *Am J Phys Anthropol.* 1968;29:39-44
31. Martin RB, Burr DB, Sharkey NA. *Skeletal Tissue Mechanics.* Springer; 1998
32. Reilly DT, Burstein AH, Frankel VH. The elastic modulus for bone. *J Biomech.* 1974;7:271-5
33. Ono A, Motoyoshi M, Shimizu N. Cortical bone thickness in the buccal posterior region for orthodontic mini-implants. *Int J Oral Maxillofac Surg.* 2008;37:334-40
34. Baumgaertel S, Hans MG. Buccal cortical bone thickness for mini-implant placement. *Am J Orthod Dentofacial Orthop.* 2009;136:230-36
35. O'Mahony AM, Williams JL, Katz JO, Spencer P. Anisotropic elastic properties of cancellous bone from a human edentulous mandible. *Clin Oral Implants Res.* 2000;11:415-21
36. Johanson NA, Charlson ME, Cutignola L, Neves M, DiCarlo EF, Bullough PG. Femoral neck bone density. Direct measurement and histomorphometric validation. *J Arthroplasty.* 1993;8:641-52
37. Ravaglioli A, Krajewski A. *Bioceramics.* London: Chapman and Hall; 1992
38. Fritz U, Diedrich P, Kinzinger G, Al-Said M. The anchorage quality of mini-implants towards translatory and extrusive forces. *J Orofac Orthop.* 2003;64:293-304

39. Owens SE, Buschang PH, Cope JB, Franco PF, Rossouw PE. Experimental evaluation of tooth movement in the beagle dog with the mini-screw implant for orthodontic anchorage. *Am J Orthod Dentofacial Orthop.* 2007;132:639–646
40. Carrillo R, Rossouw PE, Franco PF, Opperman LA, Buschang PH. Intrusion of multiradicular teeth and related root resorption with mini-screw implant anchorage: a radiographic evaluation. *Am J Orthod Dentofacial Orthop.* 2007;132:647–655
41. Proffit WR, Fields HW, Sarver DM. *Contemporary Orthodontics.* 4th ed. Mosby Elsevier; 2007
42. Sung SJ, Jang GW, Chun YS, Moon YS. Effective en-masse retraction design with orthodontic mini-implant anchorage: a finite element analysis. *Am J Orthod Dentofacial Orthop.* 2010;137:648-57
43. Ding X, Zhu XH, Liao SH, Zhang XH, Chen H. Implant-bone interface stress distribution in immediately loaded implants of different diameters: A three-dimensional finite element analysis. *J Prosthodont.* 2009;18:393-402
44. Chou HY, Muftu S, Bozkaya D. Combined effects of implant insertion depth and alveolar bone quality on periimplant bone strain induced by a wide-diameter, short implant and a narrow-diameter, long implant. *J Prosthet Dent.* 2010;104:293-300
45. Frost HM. Skeletal structural adaptations to mechanical usage (SATMU): 1. Redefining Wolff's law: the bone modeling problem. *Anat Rec.* 1990;226:403-13
46. Frost HM. Wolff's law and bone's structural adaptations to mechanical usage: an overview for clinician's. *Angle Orthod.* 1994;64:175-88

APPENDIX 1: LIMITATIONS

With regard to the bone analog, care was taken to select an analog with as many properties in common with human bone as possible. However, even though the cortical thickness, density, and modulus were comparable to human bone, certain crucial differences exist. The bone analog we used is an elastic material, not viscoelastic like human bone. Therefore, our analog would not have demonstrated the rate-dependent nature of human bone when it was loaded. Also, human bone is anisotropic and the analog we used was isotropic. In addition, our analog was more brittle than human bone, and could have incurred microdamaging during the insertion and loading of the OMIs. In human bone, this would not have incurred. Finally, our analog clearly did not have a biologic basis of cell interactions that would be present in a clinical situation.

We loaded each OMI at a force greater than a clinical load. We did this because fringes at low loads were not detectable due to the ESPI angle of incidence that we used in this study. Had we found a way to configure everything on the table so that we could have increased the angle of incidence, we could have detected strain at lower loads which would be more clinically relevant.

We loaded all OMIs only once, and steadily ramped the load. In a clinical situation, OMIs are loaded immediately and the load is expressed intermittently, or continuously over the period of weeks. Also, we did not account for the cyclic loading that bone undergoes during chewing and other functions. This cyclic loading adds additional strain to the system that our setup did not incorporate.

We were only able to measure strain as close as 2 mm to the OMI center. Ideally, we would have wanted to measure strain right at the bone-implant interface, but due to the collar on

the OMI, strain at this spot could not be visualized. Perhaps a future setup could use OMIs without collars so the bone-interface could be visualized.

APPENDIX 2: FUTURE STUDIES

A study could be conducted using the same ESPI setup as this study and the same two OMI types, but in cadaver or porcine bone. In this way, we could get a more realistic picture of how bone is strained when these two OMI types are loaded. However, this system would still lack the biology of a live bone system.

A finite element model could be used to examine the strain differences with the two OMI types. Values for human cortical and cancellous bone could be inputted, as well as the properties of these specific OMI types. In this way, we could get a better picture of how the strain is imparted to the bone and how it is distributed along the bone-implant interface.

Examining the histology of bone after loading the two OMI types would be interesting. These two OMIs could be inserted into animals, loaded at clinical levels, and the bone could be harvested to see if anything different happened on a cellular level. If Dual-Thread OMIs really cause less strain in bone than Single-Thread OMIs, we may notice more resorption and higher osteoclast counts in the Single-Thread samples.

Finally, a clinical study would be fascinating as well. The two OMI types could be placed in patients, loaded to clinical levels, and success rates could be evaluated. Particularly, it would be interesting to see this tested in patients requiring four OMIs, one in each quadrant. Single-Thread OMIs could be placed in the upper-left and lower-right of one patient and Dual-Thread OMIs placed in the upper-right and lower-left of the same patient. This could be varied patient to patient. Undergoing the same loads, it would be interesting to see if the Dual-Thread OMIs have a higher success rate.